

BL5U

Temperature-Dependent Angle-Resolved Photoemission Spectra of EuO Ultrathin Films

H. Miyazaki¹, H. Mitani^{2, 1}, T. Hajiri³, T. Ito³ and S. Kimura^{1, 4}

¹UVSOR Facility, Institute for Molecular Science, Okazaki 444-8585, Japan

²Graduate School of Engineering, Shinshu University, Nagano 380-8553, Japan

³Graduate School of Engineering, Nagoya University, Nagoya 464-8603, Japan

⁴School of Physical Sciences, The Graduate University for Advanced Studies, Okazaki 444-8585, Japan

Europium monoxide (EuO) is a ferromagnetic semiconductor with the Curie temperature (T_C) at around 70 K [1, 2]. The magnetic moment originates from the half-filled $4f$ shell of the Eu^{2+} ion with a spin-only magnetic moment of $S = 7/2$. Recently, we reported that the origin of the magnetic properties of EuO is caused by the hybridizations of the Eu $4f - O 2p$ and Eu $4f - 5d$ [3-5]. Next step is to investigate the electronic and magnetic structure of thin films of a few nanometers, which is the thickness of spin filter tunnel barriers [3]. Three dimensional angle-resolved photoemission spectroscopy (3D-ARPES) using synchrotron radiation is the most powerful technique to directly determine the electronic band structure. Using this technique we observed the change of the electronic structure across T_C .

Single-crystalline EuO ultrathin films with a thickness of about 2 nm were fabricated by a molecular beam epitaxy (MBE) method. Epitaxial growth of the single-crystalline EuO ultrathin films with the 1×1 EuO (100) patterns was confirmed by a low energy electron diffraction (LEED) method. By an *in-situ* magneto-optical Kerr rotation measurement, was about 40 K that is lower temperature than that of the bulk material. The magnetic properties and 3D-ARPES measurements were performed at the beam line 5U of UVSOR-II combined with the MBE system. The EuO ultrathin films were prepared in the growth chamber and were transferred to a 3D-ARPES chamber under UHV condition. The total energy and momentum resolutions for the ARPES measurement were set 123 meV and 0.020 \AA^{-1} at the Γ point and 45 meV and 0.014 \AA^{-1} at the X point, respectively.

Figure 1 (a) and (b) show the energy distribution curves (EDCs) of Eu $4f$ states for EuO (100) thin films with a thickness of 100 nm and 2 nm near the Γ and X points, respectively. The band width of Eu $4f$ states of the 2 nm thickness sample become narrower compare to those of the 100 nm sample. Across the ferromagnetic phase transition, the EDC with 2 nm thickness shifts to the lower binding energy side only X point. The energy shifts of Eu $4f$ states with 100 and 2 nm thickness samples are 0.3 and 0.16 eV, respectively. This result indicates that the hybridization intensity between the Eu $4f$ and other states become weaker with decreasing thickness. This is consistent with the decreasing T_C .

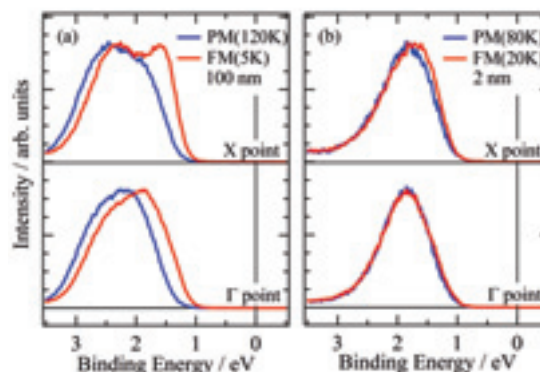


Fig. 1. Temperature-dependent energy distribution curves (EDCs) of Eu $4f$ states with a thickness of 100 nm (a) and 2 nm (b) at the Γ and X point.

- [1] N. Tsuda *et al.*, *Electronic Conduction in Oxides* (Springers College) (1976).
- [2] A. Mauger *et al.*, *J. Phys. (paris)* **39** (1978) 1125.
- [3] H. Miyazaki *et al.*, *Physica B* **403** (2008) 917.
- [4] H. Miyazaki *et al.*, *Jpn. J. Appl. Phys.* **48** (2009) 055504.
- [5] H. Miyazaki *et al.*, *Phys. Rev. Lett.* **102** (2009) 227203.
- [6] M. Müller *et al.*, *J. Appl. Phys.* **105** (2009) 07C917.

XAFS Study on the Surface Structures of the Positive Electrodes for High Power-Type Li-ion Battery Cells

M. Shikano¹, H. Kobayashi¹, H. Hori¹ and Y. Saito²

¹Research Institute for Ubiquitous Energy Devices, AIST, Ikeda, Osaka 563-8577, Japan

²Energy Technology Research Institute, AIST, Tsukuba, Ibaraki 305-8568, Japan

Introduction

Li-ion batteries are an important device because they have a higher energy density than any other type of batteries. Therefore, they are a key component for next generation vehicle such as hybrid electric vehicle (HEV), plug-in HEV (PHEV) and electric vehicle (EV). For these applications, high specific power, long calendar life and safety are very important requirements. In our previous work, degradation mechanism of Li-ion batteries has been studied by various analyzing techniques in synchrotron facilities. We concluded that the major factor of power fade was degradation of positive electrode surface [1-4]. For the degradation control of the oxide surface, we considered coating method by mechanochemical process. The coating material may protect the surface condition of positive electrode from degradation mechanism. In order to determine the coating effect, we performed X-ray absorption fine structure (XAFS) analysis of $\text{LiNi}_{1/3}\text{Mn}_{1/3}\text{Co}_{1/3}\text{O}_2$ (NMC)-based powder and obtain information on their surfaces.

Experimental

NMC was mixed with ZrO_2 (20:1 in weight), and mixture was introduced Nobilta (Type: NOB-MINI, Hosokawa Micron) to treat the surface of NMC for five minutes. Morphology of powders was observed by scanning electron microscopy (SEM). 18650-type cylindrical lithium-ion cells were manufactured using mixture of NMC, acetylene black and poly vinylidene fluoride (PVDF) as positive electrode. XAFS spectra of these powders were measured at UVSOR BL1A for Ni *L*-edge, BL4B for O *K*-edge and BL8B1 for Li *K*-edge. All measurements were performed with Total Electron Yield (TEY) technique at room temperature.

Results

According to SEM observation, submicron-sized ZrO_2 powder dispersed on the surface of NMC after Nobilta treatment. ZrO_2 powders are not dense on the surface of NMC. Morphology of powders of NMC was kept during mechanochemical process.

Obtained O *K*-edge XANES spectra of the powders are shown in Fig. 1. Peaks at 523 and 526 eV of NMC spectrum are concerned with oxygen in layered rock-salt structure and cubic structure respectively [1]. On the other hand, in case of ZrO_2 coated NMC, the peak at 523 eV seems to be enhanced by oxygen of ZrO_2 . A peak of Li_2CO_3 was not observed neither O *K*-edge XANES spectra of NMC and ZrO_2 coated NMC.

After cycle tests, degraded Li-ion cells were disassembled in order to obtain electrode materials. According to O 1s spectra of X-ray photoelectron spectroscopy (XPS), amount of Li_2CO_3 on the surfaces of positive electrodes increased after the tests similar with using $\text{LiNi}_{0.80}\text{Co}_{0.05}\text{Al}_{0.05}\text{O}_2$ positive electrodes [1]. Because XAFS measurement is unsuitable for quantitative analysis of Li_2CO_3 , comparison between XANES and XPS spectra is needed. To determine ZrO_2 -coating effect, detailed structural analysis will be studied using Ni *L*-edge spectra and so on.

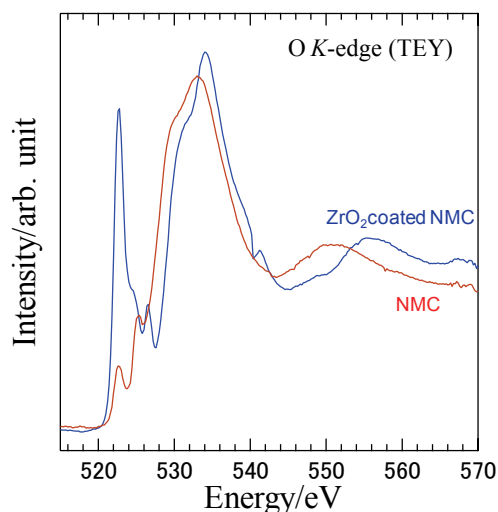


Fig. 1. O *K*-edge XANES spectra of $\text{Li}(\text{Ni}_{1/3}\text{Mn}_{1/3}\text{Co}_{1/3})\text{O}_2$ (NMC). Blue line shows ZrO_2 coated NMC.

[1] H. Kobayashi, M. Shikano, S. Koike, H. Sakaebe and K. Tatsumi, *J. Power Sources* **174** (2007) 380.

[2] M. Shikano, H. Kobayashi, S. Koike, H. Sakaebe, E. Ikenaga, K. Kobayashi and K. Tatsumi, *J. Power Sources* **174** (2007) 795.

[3] M. Rahman and Y. Saito, *J. Power Sources* **174** (2007) 889.

[4] Y. Saito and M. Rahman, *J. Power Sources* **174** (2007) 877.

Photoionization Threshold of Pyrene and Perylene on the Surface of 1-Butyl-3-Methylimidazolium Tetrafluoroborate/Water Mixture

T. Ishioka, N. Inoue, N. Fujii, K. Nishimura and A. Harata

Department of Molecular and Material Science, Kyushu University, Kasuga 816-8580, Japan

Photoionization threshold of polycyclic aromatic molecules has been measured on the surface of the mixture of 1-butyl-3-methylimidazolium tetrafluoroborate and water. The threshold energy of perylene monotonously decreased with the content of water while the value of pyrene had a minimum value around 50%. This result suggests the solvation structure of pyrene at the surface is largely different from those of perylene.

Introduction

Ionic liquids have attracted much attention due to its unique characteristics such as low melting point, high conductivity, negligible vapor pressure, and designable solubility to other solvents. Their special dielectric properties has been applied to enhance photosensitized reactions.[1]

Interfacial properties of ionic liquids also attract large interest because interface structures play a crucial role in transport kinetics and they are related directly to the applications of ionic liquids such as solvent extraction and rechargeable batteries. Interfacial characteristics of ionic liquids have been studied theoretically and experimentally by various groups. Their common conclusion on air/ionic liquid structure is that cations are present at the surface with long alkyl chains directed to the air. This conclusion implies surface molecules suffer different dielectric environment from those in bulk solutions.

The dielectric environment is directly related to the solvation conditions of solute molecules. However, it is difficult to know solvation conditions experimentally at the liquid surfaces. Photoionization is one of such methods to inform dielectric conditions at the surface because the threshold energy is lowered by the polarization energy.

In this report, photoionization thresholds of two aromatic molecules, pyrene and perylene, were measured at the surface of the mixture of 1-butyl-3-methylimidazolium tetrafluoroborate (BMIM-BF₄) and water. The water content was varied from 0-100% and the solvation characteristics were discussed.

Experimental

The monochromated synchrotron light (4-8 eV) was emitted from the chamber to the He-purged cell through an MgF₂ window. The emitted light was reflected on an Al mirror and vertically irradiated on the solution surface through a Cu-mesh electrode. The electrode was set above the liquid surface and high voltage (400 V) was applied to the electrode. The photocurrent was measured by a picoammeter.

Solution samples were prepared by spreading dilute hexane solution of pyrene or perylene on the surface of the mixture of BMIM-BF₄ and water.

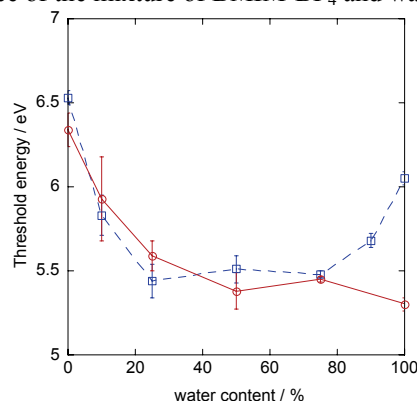


Fig. 1. Photoionization threshold energy of aromatic molecules on the surface of 1-butyl-3-methyl-imidazolium/water mixture. Solid line: perylene. Broken line: pyrene. The threshold value was derived from the mathematical fitting of $I = C(E - E_{th})^{2.5}$. I : photocurrent, C : constant, E : Photon energy.

Results and Discussion

Photoionization threshold energy (E_{th}) on the solution surface can be explained by

$$E_{th} = IP + P^+ \quad (1)$$

where IP is ionization potential in vacuum and P^+ is the polarization energy. IP s of pyrene and perylene are 7.43 eV and 6.96 eV, respectively. From Fig.1 measured photoionization threshold shows 0.9-1.9 eV lower value than each IP , indicating P^+ values. P^+ is the function of surrounding solvent properties such as dielectric constant and coordination numbers. In the case of perylene, the photoionization threshold decreases by increasing the water content showing large solvation energy by surrounding water molecule. In the case of pyrene, the threshold energy once decreases in the same manner as perylene but again increases when water content reaches above 90%. In the previous report [2], pyrene is not solvated at any content of ethylammonium nitrate. These results suggest that the solvation of pyrene is more sensitive to the structure of the surface and solvation become possible only when the dielectric condition is appropriate for pyrene. Further discussion is now in progress including molecular dynamics studies.

[1] N. Inoue, T. Ishioka and A. Harata, Chem. Lett. **38** (2009) 358.

[2] T. Ishioka, N. Inoue and A. Harata, UVSOR Activity Report **36** (2009) 58.

Exciting Phenomena of Matrix in Inorganic Phosphor

M. Ohta

Department of Material Science and Technology, Faculty of Engineering, Niigata University, Ikarashi 950-2181, Japan

It was known that rare earth ions dosed for oral administration to mouse and rat are transferred to blood vessel through the ileum and deposited its teeth and bone, which mainly consists of hydroxyapatite ($\text{Ca}_{10}(\text{PO}_4)_6(\text{OH})_2$) [1, 2]. Recently, rare earth is also useful as a contrast medium for magnetic resonance imaging, restriction enzyme, biocatalyst, and so on in fields of biochemistry, physiology, medicine, etc. However, the behavior of rare earth in the living body system remains an open question until now. We have found that Eu ion substituted Ba ion in Eu doped $\text{Ba}_{10}(\text{PO}_4)_6\text{Cl}_2$ phosphor, which matrix is apatite structure [3]. The Sm ion, Eu ion, Gd ion or Yb ion are also found to substitute easily for calcium ions in hydroxyapatite which is soaked in SmCl_3 , EuCl_3 , GdCl_3 or YbCl_3 aqueous solution, and to play on emission center.

In this study, hydroxyapatite matrix were prepared by soaking in deionized water in order to be compatible with rare earth ion doped hydroxyapatite.

Their characteristics were investigated by photoluminescent property of hydroxyapatite matrix excited by ultraviolet synchrotron orbital radiation light.

Hydroxyapatite matrix were prepared as follows: hydroxyapatite was soaked in deionized water. After

72 hr, hydroxyapatite matrix was separated from deionized water by filtration and then dried by using with infrared ray (unfired sample). The fired sample was prepared by firing the unfired sample at 1,373 K in air.

The photoluminescent property of each sample excited by ultraviolet synchrotron orbital radiation light (BL-1B) was observed by using with a multi-channel analyzer.

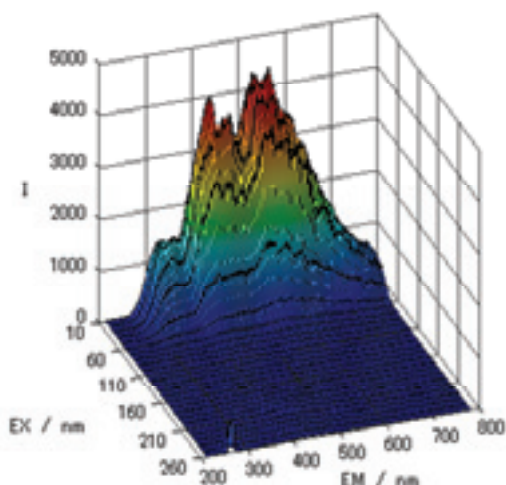
Figure 1 shows photoluminescence spectra of hydroxyapatite matrix samples excited by BL-1B. The photoluminescence spectra of both unfired and fired samples have wide length peak from 250 to 800 nm. These emission peak intensities decreased with the wave length from 10 to 100 nm of excitation wave length. This phenomenon is thought to be due to the multi-electron excitation.

[1] S. Hirano, K. T. Suzuki, *Environ. Health Perspect.* **104** (Supplement 1) (1996) 85.

[2] K. Kostial, B. Kargacin, M. Lendeka, *Int. J. Radiat. Biol. Relat. Stud. Phys. Chem. Med.* **51** (1987) 139.

[3] M. Sato, T. Tanaka, M. Ohta, *J. Electrochem. Soc.* **141** (1994) 1851.

Unfired



Fired

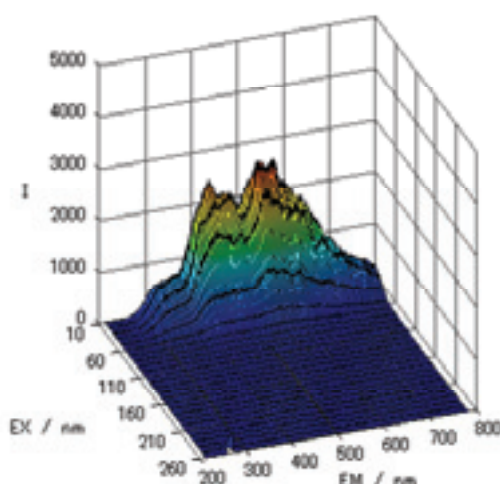


Fig. 1. Photoluminescent spectra of hydroxyapatite matrix excited by ultraviolet synchrotron orbital radiation light.

Field Effect on the Electronic States of Oligothiophene Thin Films Studied by Fluorescence-Yield X-Ray Absorption Spectroscopy

H. S. Kato¹, H. Yamane², N. Kosugi², M. Kawai^{1,3}

¹RIKEN (The Institute of Physical and Chemical Research), Wako 351-0198, Japan

²Institute for Molecular Science, Okazaki 444-8585, Japan

³Department of Advanced Materials Science, University of Tokyo, Kashiwa 277-8501, Japan

Introduction

In order to extend new functionality of electronic devices, the molecular devices have recently been investigated with great efforts. The organic field effect transistor (OFET) is a typical molecular device that controls electric conductivity by injection of carriers into the organic thin film under the applied electric field. Since the organic materials consist of molecular units having their own molecular orbitals, it is not clear that the energy diagram of OFET is exactly the same as that of inorganic semiconductors, i.e., band bending at the interface in the semiconductor side. Therefore, the direct observation of electronic states in the organic thin films under operative conditions has been required.

In this study, we aim to elucidate the electronic state of organic thin films in OFET under the electric field. The fluorescence-yield X-ray absorption spectroscopy (FY-XAS) should be a promising method for detection of inner electronic states of organic devices, because the fluorescent X-rays have a long penetration depth of about 100 nm in most of materials even for the soft X-ray region. In addition, X-rays are not disturbed by applied electric fields, and have different characteristics from the emitted electrons. Thus, we have attempted to utilize FY-XAS for investigation of inner electronic states of OFETs.

Experimental

To investigate the electronic states of OFET, α,ω -dihexylsexithiophene (DH6T) thin films on the SiO₂-covered Si substrates were fabricated at RIKEN. It is known that DH6T FET shows as *p*-type-like I-V property. The fabricated DH6T films were covered homogeneously with a thin Au electrode (25 nm thick). By the incident angle dependence of XAS spectra, we confirmed that the orientation of molecules in the DH6T thin film is not change significantly even after the Au electrode deposition.

The FY-XAS measurements were performed at the BL3U beamline of the UVSOR facility in IMS. The samples were set in a BL3U end-station through a sample-entry system. The fluorescence intensities were measured using a retarding field detector consisting of the MCP system.

Results and Discussion

Figure 1(a) shows the gate bias dependence of the C K-edge FY-XAS spectra of the DH6T films (17 nm thick), in which the spectra at the bias of 0 V and -90 V are plotted. The bias voltage was applied with a

square wave (7 Hz) synchronized to the veto signals to the two fluorescence signal counters for each of the bias conditions, which enabled reliability of the difference spectrum. Figure 1(b) shows the spectral change at the biases from 0 V to -90 V, in which the sharp peaks at the photon energies around 285 eV on the original spectra are absent, while the broader components at 288 and 291 eV appears in the difference spectrum. In Fig. 1(b), the spectral change of a DH6T-lacked sample at the same bias conditions is also shown, and no meaningful spectral changes are confirmed. These results clearly show that the observed spectral change is caused by an electronic state modification in the DH6T thin films under the applied bias. From the bias dependence of the FY-XAS spectra, the spectral change is considered as a result of distorted molecular orbitals by the applied electric field.

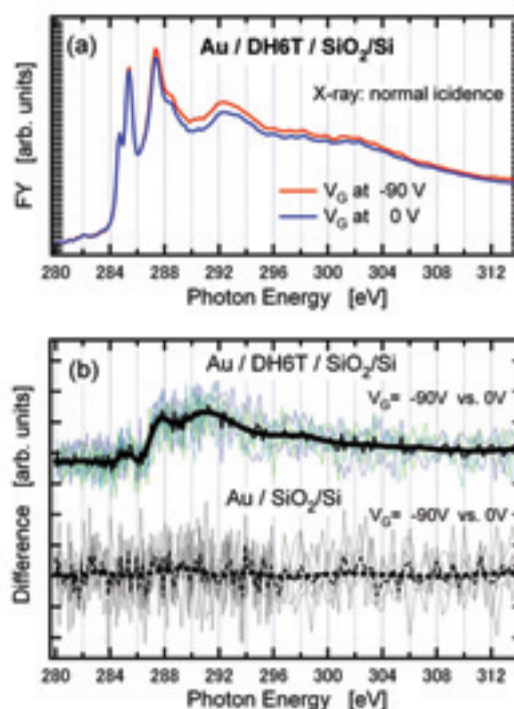


Fig. 1. Bias dependence of the C K-edge fluorescence-yield XAS spectra of the Au-covered DH6T films (17 nm thick) measured at normal incidence geometry: (a) the spectra at the biases of 0 V and -90 V, (b) spectral changes at the biases from 0 V to -90 V (solid lines) as compared with that of a DH6T-lacked sample (broken lines).

Temperature-Dependent Magnetic Circular Dichroism Spectra of Ferromagnetic Semiconducting EuO Thin Films

H. Miyazaki¹, H. Mitani^{2,1}, T. Hajiri³, T. Ito³, Y. Takagi^{4,5}, T. Nakagawa^{4,5}, Y. Yamamoto⁴
T. Yokoyama^{4,5} and S. Kimura^{1,5}

¹*UVSOR Facility, Institute for Molecular Science, Okazaki 444-8585, Japan*

²*Graduate School of Engineering, Shinshu University, Nagano 380-8553, Japan*

³*Graduate School of Engineering, Nagoya University, Nagoya 464-8603, Japan*

⁴*Department of Materials Molecular Science, Institute for Molecular Science, Okazaki 444-8585, Japan*

⁵*School of Physical Sciences, The Graduate University for Advanced Studies, Okazaki 444-8585, Japan*

Europium monoxide (EuO) is a ferromagnetic semiconductor with the Curie temperature (T_C) at around 70 K [1, 2]. In the electron doping case by Eu excess or substitution of Eu^{2+} by Gd^{3+} or La^{3+} ion, T_C increases up to 200 K and the electrical resistivity drops twelve-order of magnitude below T_C originating in a metal-insulator transition (MIT) [2-4]. To reveal the origin of these physical properties of EuO, it is important to clarify the relation of the electronic structure to the magnetic property. Soft X-ray Magnetic Circular Dichroism (XMCD) is a powerful technique to determine a magnetic configuration of electronic structure. Using this technique we observed the electronic structure of the Eu 4*f* states under a magnetic field.

Single-crystalline EuO thin films with a thickness of about 50 nm were fabricated by a molecular beam epitaxy (MBE) method. Epitaxial growth of single-crystalline EuO thin films with the 1 × 1 EuO (100) patterns was confirmed with low energy electron diffraction (LEED) and reflection high energy electron diffraction (RHEED) methods. T_C measured with a Superconducting QUantum Interference Device (SQUID) magnetometer was 71 K [5]. *In situ* Eu *M*-edge X-ray adsorption spectra (XAS) and XMCD measurements were performed using a total electron yield mode at the bending magnet beamline 4B of UVSOR-II combined with the MBE system. The EuO thin films were prepared in the growth chamber and were transferred to a superconducting magnet chamber under UHV condition.

Figure 1 shows the temperature-dependent Eu M_5 XMCD spectra of an EuO (100) thin film recorded at the magnetic field H of ± 1 T. The magnetic field was applied perpendicular to the sample surface. The XMCD spectrum, which is obtained by the subtraction of the XAS spectrum of $H = -1$ T from that of 1 T, is in good agreement with previously results and theoretical spectrum for a Eu^{2+} ion with $L = 0$ and $S = 7/2$ [6, 7]. The inset of Fig.1 shows the temperature dependence of the integration of the MCD spectrum and the magnetization curve measured by SQUID. The MCD signals are in good agreement with the magnetization curve.

To summarize, we succeeded to measure temperature dependent XMCD spectra of single-crystalline EuO (100) thin films. The method is a good probe to investigate the electronic structure of each element. The detailed analysis and further study on the magnetic electronic structure of EuO thin films are in progress.

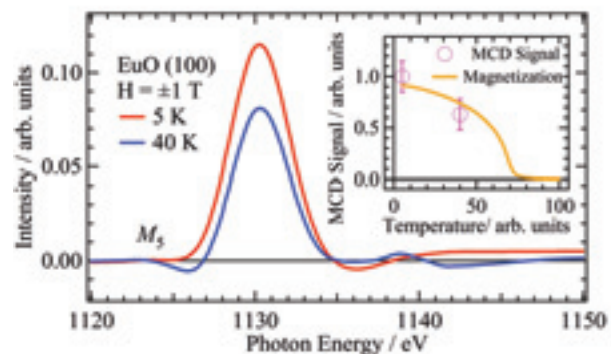


Fig. 1. Temperature-dependent Eu M_5 XMCD spectra of EuO thin films recorded at ± 1 T. The inset shows the temperature dependence of the integration of the MCD spectrum and the magnetization curve.

- [1] N. Tsuda *et al.*, *Electronic Conduction in Oxides* (Springers College) (1976).
- [2] A. Mauger *et al.*, *J. Phys. (paris)* **39** (1978) 1125.
- [3] Y. Shapira, S. Foner and T. B. Reed, *Phys. Rev. B* **8** (1973) 2299 ; **8** (1973) 2316.
- [4] H. Miyazaki *et al.*, *Appl. Phys. Lett.* (2010) *in press*.
- [5] H. Miyazaki *et al.*, *Jpn. J. Appl. Phys.* **48** (2009) 055504.
- [6] J. Holroyd *et al.*, *J. Appl. Phys.* **95** (2004) 6571.
- [7] J. B. Goedkoop *et al.*, *Phys. Rev. B* **37** (1988) 2086.

Magnetism of Mn and Fe Ultrathin Films on Bi(0001)

T. Nakagawa, Y. Takagi, I. Yamamoto and T. Yokoyama

Department of Material Molecular Science, Institute for Molecular Science, Okazaki
444-8585, Japan

Elements with large atomic number have strong spin orbit coupling (SOC). Their compounds are used as magnetic materials since they show large magnetic anisotropy due to SOC. Bi is the largest atom with stable isotopes and one of the Bi-Mn compounds is well known as a magnetic material, which shows large uniaxial anisotropy derived from SOC by Bi and exhibits a perpendicular magnetization and a large magneto-optical constant. Since the large SOC of Bi is a good candidate to give strong anisotropy magnetic properties, we have studied the magnetic properties of Mn and Fe on Bi(0001) surface using x-ray magnetic circular dichroism (XMCD).

XMCD experiments were carried out at BL4B, which delivers circular polarized light. The end station was an ultrahigh vacuum chamber equipped with a superconductive magnet (5 T) and a low temperature insertion of 5 K [1]. Fe and Mn were deposited onto a Bi(0001) crystal, which was cleaned by Ar ion sputtering and annealing. After the deposition at 300 K, the samples were annealed up to 400 K to obtain good surface ordering, as judged by low energy electron diffraction (shown in Fig.1). The Mn and Fe coverages were 0.5 ML (1ML = $1.11 \times 10^{19} \text{ m}^{-2}$), determined from a calibration of the evaporators. The Mn/Bi(0001) and Fe/Bi(0001) exhibits similar diffraction patterns ($n \times 1$) structure, $n = 3$ and 4).

Figure 1 shows an XMCD spectrum for Mn/Bi(0001) at $T_s = 5 \text{ K}$ and $H = 5 \text{ T}$. The x-ray absorption spectra (XAS) taken at $H = \pm 5 \text{ T}$ are almost identical, resulting in no magnetic signal. Thus the Mn/Bi(0001) is not ferromagnetic even at 5 K.

Figure 2 shows XMCD result for Fe/Bi(0001) at $T_s = 5 \text{ K}$ and $H = \pm 5 \text{ T}$. Figure 2(a) shows magnetization curves for the photon incidence angle of 55° (GI) and 0° (NI) from the surface normal. The magnetization in the case of GI is almost saturated at $H = 2.5 \text{ T}$, while the sample with the magnetic field normal to the surface is not magnetically saturated even at $H = 5 \text{ T}$. Therefore the magnetization easy axis is within the film plane. The evaluated effective spin magnetic moment (m_s^{eff}) and orbital magnetic moment (m_{orb}) for Fe are $1.40 \mu_B$ and $0.11 \mu_B$, respectively. Its spin magnetic moment is much smaller than that for bulk Fe ($2.2 \mu_B$). The reduced magnetic moment could be due to the alloying of Fe with Bi. The ratio between the spin and orbital magnetic moments ($m_{\text{orb}}/m_s^{\text{eff}}$) is 0.08, larger than that for bulk Fe. The obtained anisotropy constant is $\sim 100 \mu\text{eV/atom}$.

In conclusion, the Mn(0.5 ML)/Bi(0001) surface

does not show ferromagnetism even at $T_s = 5 \text{ K}$ in contrast to the MnBi alloy. This is probably ascribed to different crystalline structures. The Fe(0.5 ML)/Bi(0001) is ferromagnetic and shows an in-plane magnetization easy axis and its anisotropy constant is $100 \mu\text{eV/atom}$.

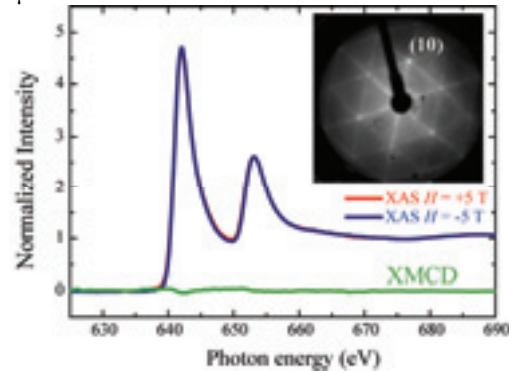


Fig. 1. XAS and XMCD spectra at Mn L edges for Mn(0.5 ML)/Bi(0001) surface. The inset shows a corresponding diffraction pattern.

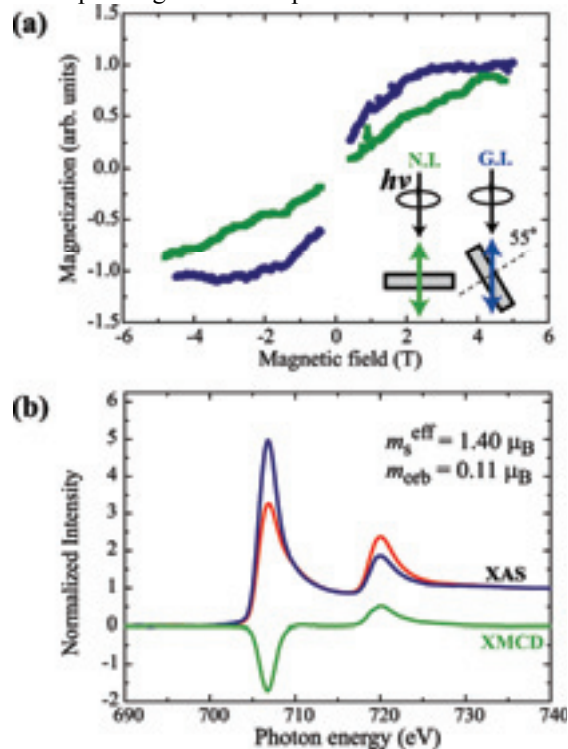


Fig. 2. (a) Magnetization curves taken at Fe L_3 edge on Fe(0.5 ML)/Bi(0001) for the normal incidence (N.I.) and grazing incidence (G.I.) (b) XAS and XMCD spectra at Fe L edges at $H = 5 \text{ T}$.

[1] T. Nakagawa, Y. Takagi, Y. Matsumoto and T. Yokoyama, Jpn. J. Appl. Phys. **47** (2008) 2132.

Oscillatory Magnetic Anisotropy in Fe/Ag(116)

M. Przybylski¹, F. Yildiz¹, U. Bauer¹, Y. Takagi², I. Yamamoto², T. Nakagawa²
and T. Yokoyama²

¹Max-Planck-Institut für Mikrostrukturphysik, Weinberg 2, 06120 Halle, Germany

²Institute for Molecular Science, Okazaki 444-8585, Japan

Magnetic thin films deposited on vicinal single crystal surfaces are well known to exhibit double loop hysteresis along the magnetically hard axis within the surface plane, in which the separation between the two loops is called a shift field H_s . Very recently, Li *et al.* [1] discovered a very interesting phenomenon in Fe/Ag(1 1 10), whereby the shift field measured along the \perp step direction (hard axis within the film plane) shows an oscillatory structure as a function of Fe thickness at 5 K, while room temperature measurements give a monotonic increase with Fe thickness. The oscillation period is ~ 5.7 ML, which might correspond to the quantum well state. The finding should be ascribed to the oscillatory change in magnetocrystalline or magnetoelastic anisotropies. In this work, we have investigated magnetic anisotropy of Fe/Ag(116) from the view point of microscopic magnetic orbital magnetic moments by recording angle dependent Fe L-edge x-ray magnetic circular dichroism (XMCD). The reason for the replacement of the substrate from Ag(1 1 10) to Ag(116) is for possible enhancement of the oscillation amplitude.

An Ag(116) single crystal was cleaned by repeated cycles of Ar⁺ sputtering and annealing, and the surface cleanliness and order were verified by LEED/AES and x-ray absorption spectroscopy. The LEED pattern exhibits very beautiful double spots typical to vicinal surfaces. Fe was deposited on clean Ag(116) at room temperature to provide wedge-shaped or flat films.

In situ Fe L-edge XMCD spectra were recorded with a total electron yield mode from a sample drain current. The magnetic field applied with a JANIS UHV superconducting magnet [2] was ± 5 or ± 0 T, and the sample temperature was 5.0 K. Angle dependence was examined to derive components of magnetic moments along \perp surface, \parallel step, and \perp step (\parallel surface). The magnetization along any direction was confirmed to be well saturated at ± 5 T.

Figure 1 shows the angle dependent XMCD spectra of 7.2 and 7.4 ML Fe/Ag(116) at remanence magnetization. By analyzing the angle dependence, the remanence magnetization vectors can be obtained, which are depicted in the figure. At 7.4 ML the remanence magnetization is parallel to the step, while at 7.2 ML it is almost perpendicular to the surface. An abrupt spin reorientation transition is confirmed around 7.3 ML.

The orbital magnetic moments m_{orb} were evaluated

by using the well established XMCD sum rule. The m_{orb} values along \parallel surface and \parallel step shows gradual monotonic decrease as the Fe thickness. On the contrary, those along \perp step (\parallel surface) exhibits two sharp minima around 5 and 11 ML. The magnetic anisotropy within the surface plane is maximized at 5 and 11 ML. The period of ~ 6 ML agrees well with the previous value [1]. Note that in the previous experiments using magneto-optical Kerr effect measurements, thinner ranges below ~ 10 ML Fe were not investigated due to the spin reorientation transition to perpendicular magnetization as in Fig. 1. In this work, the presence of the oscillatory behavior is newly confirmed even in thinner Fe films exhibiting perpendicular magnetization.

Conclusively, the oscillatory behavior of the shift field is ascribed to the periodic change of the orbital magnetic moment along the \perp step (\parallel surface) direction.

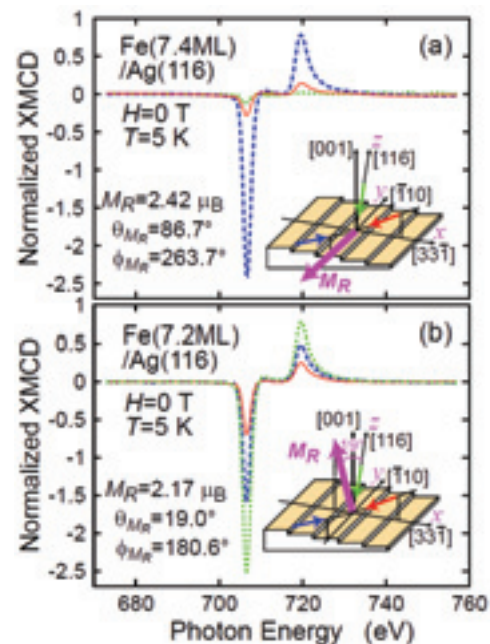


Fig. 1. Fe L-edge XMCD spectra of (a) 7.4 ML and (b) 7.2 ML Fe/Ag(116) at $T=5.0$ K and $H=0$ T. Determined remanence magnetizations are depicted in insets.

[1] J. Li, M. Przybylski, F. Yildiz, X. D. Ma and Y. Z. Wu, Phys. Rev. Lett. **102** (2009) 207206.

[2] T. Nakagawa, Y. Takagi, Y. Matsumoto and T. Yokoyama, Jpn. J. Appl. Phys. **47** (2008) 2132.

Magnetic Films Formed on the Si Substrates with Passivation Layers

Y. Takagi^{1,2}, K. Isami², I. Yamamoto¹, T. Nakagawa^{1,2} and T. Yokoyama^{1,2}

¹Institute for Molecular Science, Okazaki 444-8585, Japan

²The Graduate University for Advanced Studies, Okazaki 444-8585, Japan

We report on a study of magnetic films formed on the Si substrate by means of X-ray magnetic circular dichroism (XMCD) at BL4B, equipped with a superconducting magnet system.

The sample preparation and XMCD measurement were carried out in a UHV chamber. A Si(111) wafer was degassed in the UHV chamber over 5 h and was flashed at 1200 °C. After these cleaning procedures, the Si(111) surface exhibits a 7×7 reconstruction. We used Si(111)- $\sqrt{3}\times\sqrt{3}$ Ag and silicon nitride (SiN) surfaces as passivation layers. The former was prepared by depositing silver of 1 monolayer (ML) on the Si(111)- 7×7 substrate at 450 °C. The latter was obtained by exposing to low energy (200 eV) N^+ bombardment with pressure (2×10^{-6} Torr) at room temperature (RT) for 20 min and subsequently flashing at 1200 °C. The ordering and cleanness of the surfaces were checked by low energy electron diffraction and Auger electron spectroscopy. Pure iron (99.99%) was evaporated from an electron-beam evaporator. In this report, we define a unity monolayer as atomic concentration of Fe of 7.83×10^{14} atoms/cm², which corresponds to the Si atomic density of the Si(111)- 1×1 surface.

Figure 1 gives XMCD spectra of Fe L_{III,II}-edge measured under the magnetic field of ± 5 T at a sample temperature of 5 K. The magnetization of the Fe film on Si(111)- $\sqrt{3}\times\sqrt{3}$ Ag is stronger than that on Si(111)- 7×7 substrate. Regarding bulk iron silicide, the magnetic moment decreases with increasing the composition ratio of Si to Fe and becomes almost zero when the stoichiometry of Fe:Si is 1:1. The XMCD results indicate that the films contain the Fe-rich silicide and the $\sqrt{3}\times\sqrt{3}$ Ag layer on Si(111) suppresses the reactivity of the substrate with Fe. On the other hand, the spin magnetic moment of the Fe film on SiN obtained by XMCD is $2.17\mu_B$, which is almost the same as the bulk Fe of $2.2\mu_B$. The passivation effect of SiN is stronger than that of the $\sqrt{3}\times\sqrt{3}$ Ag layer and the reaction between Fe and Si is quenched almost completely.

To investigate the passivation effect to annealing, we have measured the XMCD spectra for the Fe films grown on the substrates held at 200 °C (Fig. 2). For the film on $\sqrt{3}\times\sqrt{3}$ Ag layer, the magnetization is quite small because the silicidation is enhanced with increasing growth temperature. On the other hand, the decrease in the magnetization on SiN is much smaller than that on $\sqrt{3}\times\sqrt{3}$ Ag. The passivation effect of SiN is more effective than that of $\sqrt{3}\times\sqrt{3}$ Ag in the heating deposition at elevated temperature.

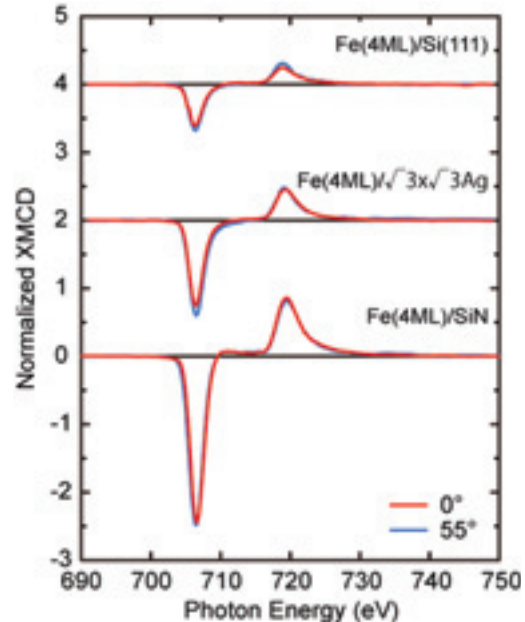


Fig. 1. Fe L_{III,II}-edge XMCD spectra of 4ML Fe film deposited on Si(111)- 7×7 , Si(111)- $\sqrt{3}\times\sqrt{3}$ Ag, SiN substrates at RT, taken at $T=5$ K and $H=\pm 5$ T, with x-ray incident angles $\theta=0^\circ$ (red line) and $\theta=55^\circ$ (blue line).

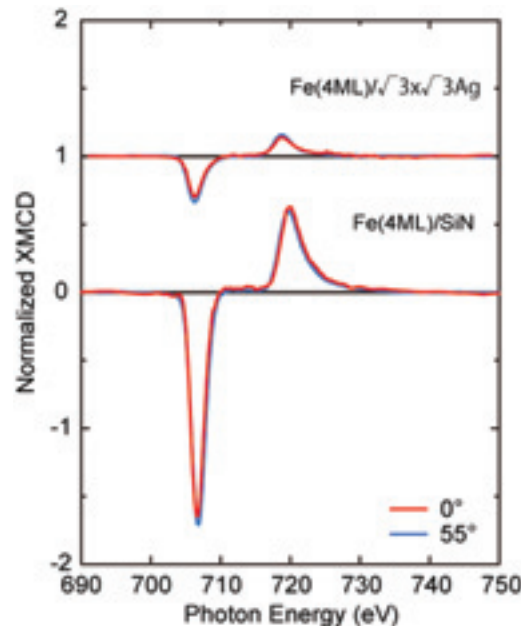


Fig. 2. Fe L_{III,II}-edge XMCD spectra of 4ML Fe films deposited on Si(111)- $\sqrt{3}\times\sqrt{3}$ Ag and SiN at 200 °C, taken at $T=5$ K and $H=\pm 5$ T, with x-ray incident angles $\theta=0^\circ$ (red line) and $\theta=55^\circ$ (blue line).

Magnetic Property of Manganese Phthalocyanine on Ferromagnetic Thin Films Studied by XMCD

I. Yamamoto¹, K. Eguchi², T. Nakagawa^{1,2}, Y. Takagi^{1,2} and T. Yokoyama^{1,2}

¹Department of Molecular Structure, Institute for Molecular Science, Okazaki 444-8585, Japan

²School of Physical Science, The Graduate University for Advanced Studies (SOKENDAI), Okazaki 444-8585, Japan

To realize molecular spintronic devices, it is important to understand the magnetic coupling between molecules and magnetic metal surfaces as well as the magnetization of organic materials. Metal phthalocyanines (Pc's) have attracted much interest due to their characteristic electronic, optical and magnetic properties. Manganese phthalocyanine (MnPc) is one of the interesting molecules because only β -phase MnPc is known as a ferromagnet among undoped Pc's [1]. Isolated MnPc in Ar matrix has an orbital degenerate ground state, which leads to large orbital magnetic moments [2]. Moreover, the epitaxial MnPc film grown on H-Si(111) has a large perpendicular magnetic anisotropy [3]. In this study, we have investigated magnetic properties of MnPc thin films on ferromagnetic metal films.

Co films were prepared on a clean Cu(001) substrate by the e-beam evaporation method at room temperature (RT). Purified MnPc was deposited at RT by sublimation. The Co L - and Mn L -edge XMCD measurements were done using a system (JANIS: 7THM-ST-UHV) with a superconducting magnet and a liq. He cryostat. The XMCD spectra were recorded with reversal of the magnetic field. The XMCD measurements were done at 5 K.

Figure 1 shows magnetization curves for MnPc/Co(3 ML)/Cu(001) recorded with the Co L_3 intensity. By depositing MnPc monolayer, the anisotropic magnetic field H_a decreases from 6.2 to 3.2 T, implying that the MnPc-Co interface favors perpendicular magnetization, though the magnetization easy axis is still in-plane. The effective magnetic anisotropy energy K^{eff} were obtained as -230 and -70 $\mu\text{eV}/\text{atom}$ for the bare Co (3 ML) and the MnPc (1 ML) covered films, respectively.

The Mn L -edge XMCD spectra for various MnPc thickness on Co(3 ML)/Cu(001) measured at incident angle $\theta_i=55^\circ$ from the surface normal and at 5 K are shown in Fig. 2. For the monolayer MnPc film, the Mn L -edge XMCD displays the same sign as the Co L -edge XMCD. The Mn L_3 XMCD intensity at 0.3 T is about 80 % of the saturation value, which coincides with the magnetization curves recorded with the Co L_3 intensity. Thus the magnetization behavior of the Mn atom in phthalocyanine is the same as that of the ferromagnetic Co film. These results suggest that the presence of a ferromagnetic exchange coupling between Mn and Co. Above 2 ML, however, the Mn

L_3 XMCD intensity at 0.3 T is not consistent with Co L_3 intensity, and the magnetization behavior of the Mn atom is paramagnetic. In addition, the Mn L_2 XMCD sign is same negative as the Mn L_3 , indicating an intrinsic large orbital magnetic moment of MnPc. Therefore substantial interaction is present at the MnPc-Co interface, resulting in the ferromagnetic exchange coupling between MnPc and Co.

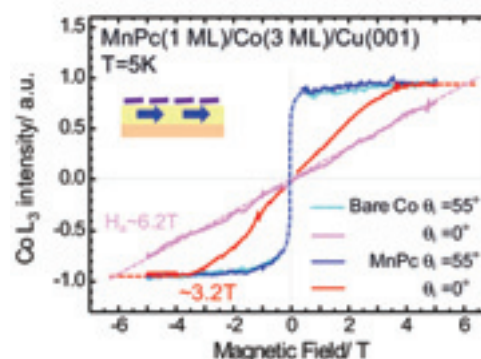


Fig. 1. Magnetization curves for bare Co (3 ML) and MnPc(1 ML) covered films at 5 K with $\theta=0^\circ$ (surface normal) and 55° .

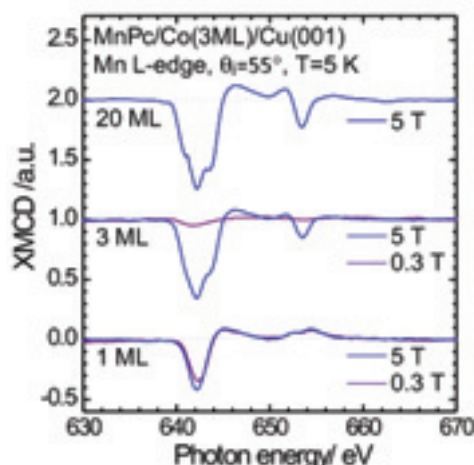


Fig. 2. Mn L -edge XMCD spectra for various MnPc thickness on Co(3 ML)/Cu(001) measured at incident angle $\theta_i=55^\circ$ from the surface normal and at 5 K.

[1] H. Miyoshi *et al.*, Bull. Chem. Soc. Jpn. **46** (1973) 2724.

[2] B. E. Williamson *et al.*, J. Am. Chem. Soc. **114** (1992) 2412.

[3] H. Yamada *et al.*, J. Chem. Phys. **108** (1998) 10256.

A Topological Metal at the Surface of an Ultrathin BiSb Alloy Film

T. Hirahara¹, Y. Sakamoto¹, Y. Saisyu¹, H. Miyazaki², S. Kimura²,
T. Okuda^{3,4}, I. Matsuda⁴, S. Murakami⁵ and S. Hasegawa¹

¹Department of Physics, University of Tokyo, Tokyo 113-0033, Japan

²UVSOR Facility, Institute for Molecular Science, Okazaki 444-8585, Japan

³Hiroshima Synchrotron Radiation Center, Hiroshima University,
Higashi-Hiroshima 739-0046, Japan

⁴Synchrotron Radiation Laboratory, ISSP University of Tokyo, Kashiwa 277-8581, Japan

⁵Department of Physics, Tokyo Institute of Technology, Tokyo 152-8551, Japan

Recently there has been growing interest in *topological insulators* or the *quantum spin Hall (QSH) phase*, which are insulating materials with bulk band gaps but have metallic edge states that are formed topologically and robust against any non-magnetic impurity [1]. In a three-dimensional material, the two-dimensional surface states correspond to the edge states (topological metal) and their intriguing nature in terms of electronic and spin structures have been experimentally observed in bulk $\text{Bi}_{1-x}\text{Sb}_x$ single crystals [2-4]. However, if we want to investigate the transport properties of these topological metals, high purity samples as well as very low temperature will be needed because of the contribution from bulk states or impurity effects. In a recent report, it was also shown that an intriguing coupling between the surface and bulk states will occur [5] for the single crystal BiSb. A simple solution to this bothersome problem is to prepare a topological metal on an ultrathin film, in which the surface-to-bulk ratio is drastically increased.

Therefore in the present study, we have investigated if there is a method to make an ultrathin $\text{Bi}_{1-x}\text{Sb}_x$ film on a semiconductor substrate. From reflection high-energy electron diffraction observation, it was found that single crystal $\text{Bi}_{1-x}\text{Sb}_x$ films ($0 \leq x < 0.32$) as thin as ~ 30 Å can be prepared on Si(111)-7x7. The core level spectra of Bi *5d* and Sb *4d* showed that the stoichiometry of ratio of Bi and Sb is fairly homogeneous over the whole sample. Figure 1 represents the Fermi surface of 40 Å thick $\text{Bi}_{0.92}\text{Sb}_{0.08}$ (a) and $\text{Bi}_{0.84}\text{Sb}_{0.16}$ (b) films mapped by angle-resolved photoemission spectroscopy. The basic features of the electronic structure of these surface states were shown to be the same as those found on bulk surfaces, meaning that topological metals can be prepared at the surface of an ultrathin film. Finally, the transport properties of such films were characterized by *in situ* monolithic micro four-point probes [6]. The temperature dependence of the resistivity for the $x=0.1$ samples was insulating when the film thickness was 240 Å. However, it became metallic as the thickness was reduced down to 30 Å, indicating surface-state dominant electrical conduction for the thinnest films. Therefore by investigating the properties of these ultrathin BiSb alloy films, it can be expected that we can verify the

intriguing topological nature of the edge states.

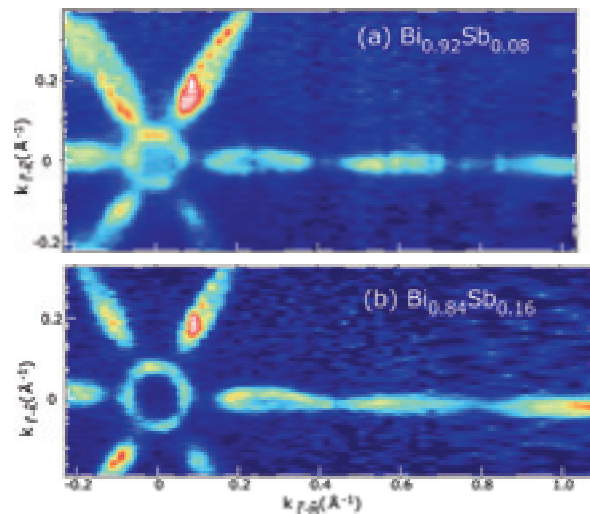


Fig. 1. The Fermi surface mapped by ARPES at 10 K for 40 Å thick $\text{Bi}_{0.92}\text{Sb}_{0.08}$ (a) and $\text{Bi}_{0.84}\text{Sb}_{0.16}$ (b) films, respectively. A circularly polarized light was used at the photon energy of 28 eV.

- [1] L. Fu and C. L. Kane, Phys. Rev. B **76** (2007) 045302.
- [2] D. Hsieh, D. Qian, L. Wray, Y. Xia, Y. S. Hor, R. J. Cava and M. Z. Hasan, Nature **452** (2008) 970.
- [3] D. Hsieh, Y. Xia, L. Wray, D. Qian, A. Pal, J. H. Dil, J. Osterwalder, F. Meier, G. Bihlmayer, C. L. Kane, Y. S. Hor, R. J. Cava and M. Z. Hasan, Science **323** (2009) 919.
- [4] A. Nishide, A. A. Taskin, Y. Takeichi, T. Okuda, A. Kakizaki, T. Hirahara, K. Nakatsuji, F. Komori, Y. Ando and I. Matsuda, Phys. Rev. B. **81** (2010) 041309(R).
- [5] A. A. Taskin and Y. Ando, Phys. Rev. B **80** (2009) 085303.
- [6] T. Tanikawa, I. Matsuda, R. Hobara and S. Hasegawa, e-Journal of Surface Science and Nanotechnology, **1** (2003) 50.

NEXAFS Study on the Synchrotron Radiation Effect on the Local Structure of Highly-Hydrogenated Diamond-Like Carbon Film

K. Kanda and S. Matsui

Laboratory of Advanced Science and Technology for Industry, University of Hyogo, Kamigori, Hyogo, 678-1205 Japan

DLC films are generally known to be etched by the exposure to the synchrotron radiation (SR) in the soft x-ray region under oxygen gas atmosphere, while they are not etched in the absence of oxygen gas.¹⁾ Recently, the irradiation of soft x-ray against highly-hydrogenated DLC (H-DLC) films in the vacuum are reported to bring about the departure of hydrogen and increase in the film density, hardness and refractive index.²⁾ In the present study, we investigated the SR effect on the highly-hydrogenated DLC film in the vacuum. Highly-hydrogenated DLC thin films were deposited on Si wafer with 200 nm thickness by amplitude-modulated RF plasma-CVD method. The irradiation of SR against DLC films was carried out at BL-6 of NewSUBARU.³⁾ The SR at the BL-6 sample stage had a continuous spectrum from IR to soft X-ray, which was lower than 1 keV.

The hydrogen content in the DLC film was determined with the combination of ERDA/RBS techniques. It decreases exponentially with a soft X-ray exposure dose in the high-hydrogenated DLC film. Thus, the departure of the hydrogen was observed from high-hydrogenated DLC films, while was not observed from the low-hydrogenated DLC film by soft X-ray irradiation.

The measurement of NEXAFS spectra was performed at BL8B1 of UVSOR. X-ray beam in the desired energy range was extracted using monochromator equipped with a 540 lines/mm laminar grating which had a 15 m radius. The carbon K edge absorption NEXAFS spectra were measured in the energy range of 275–320 eV. The energy resolution of x-ray beam was estimated to be ≈ 0.5 eV in full width at half maximum with slit width of 20 μm . The reading of monochromator was calibrated against the pre-edge resonance corresponding to the carbon $1s \rightarrow \pi^*$ transition appeared at 285.3 eV in the NEXAFS spectrum of graphite. The detection of electrons coming from the sample was performed in the total electron yield mode. The intensity of incident x-ray was measured by detecting the photocurrent from a gold film. The NEXAFS spectrum was given by the ratio of the photocurrent from the sample to that from the gold film.

Observed NEXAFS spectra are shown in Fig. 1. In the NEXAFS spectrum of as-deposited highly-hydrogenated DLC film, three peaks (orange arrow) were observed in the 283–308 eV. These peaks were not observed in the NEXAFS spectra of typical DLC films. In addition, these peaks were disappeared after the SR irradiation of 3600 mA·h. Therefore,

these peaks can be regarded to generate from the storage of hydrogen, which was departed by the SR exposure.

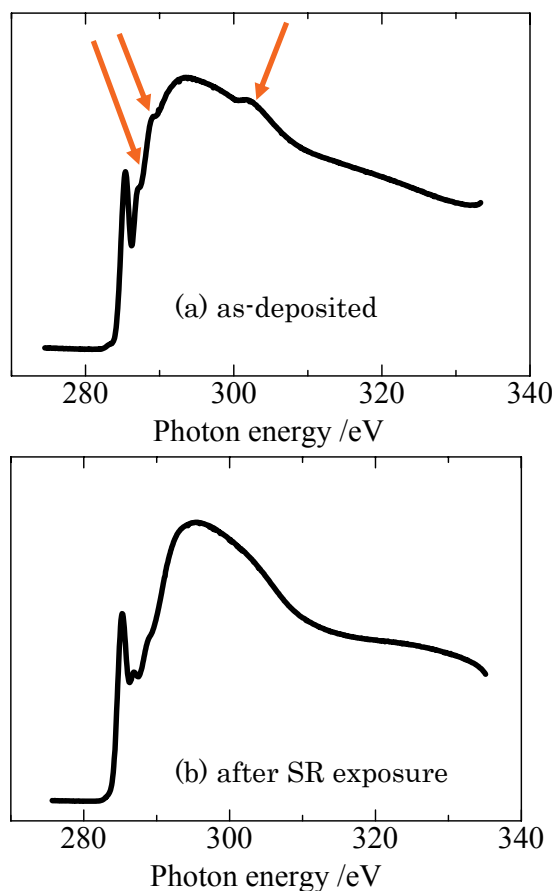


Fig. 1. C K-edge NEXAFS spectra of high-hydrogenated DLC films: (a) as-deposited, and (b) after SR exposure of 3600 mA·h.

[1] H. Kyuragi and T. Urisu, *Appl. Phys. Lett.* **50** (1987) 1254.

[2] H. Matsuura, S. Okubo, K. Oda and T. Ushiro, *SEI Technical Review* **171** (2007) 39 (Japanese).

[3] K. Kanda, T. Ideta, Y. Haruyama, H. Ishigaki and S. Matsui, *Jpn. J. Appl. Phys.* **42** (2003) 3983.

Electronic Structure and Molecular Orientation of Picene Film

D. Ikeda¹, S. Hosoumi², R. Tateishi¹, T. Nishi^{2,3}, S. Nagamatsu³, N. Ueno^{1,2} and S. Kera^{1,2,3}

¹ Faculty of Engineering, Chiba University, Chiba 263-8522, Japan

² Graduate School of Advanced Integration Science, Chiba University, Chiba 263-8522, Japan

³ Institute for Molecular Science, Okazaki 444-8585, Japan

Picene has a larger band gap (3.3eV) than polyacene compounds such as pentacene (1.8eV) which has been widely researching as an organic device material. Recently picene has a paid attention to as a new candidate for organic device material because of high mobility (3cm²/Vs) and superconductivity (Tc~20K) with K doping [1].

In this study, we measured the electronic structure of picene film prepared on highly oriented pyrolytic graphite (HOPG) by angle-resolved ultraviolet photoelectron spectroscopy (ARUPS). ARUPS has been known as a powerful technique to obtain crucial information on electronic band structure for various kinds of materials. Moreover, for organic thin films, information on the geometrical structure of the thin films can be discussed in accordance with a quantitative analysis of the ARUPS intensity using photoelectron scattering theory [2].

Experimental

A cleaved HOPG (ZYA grade) is used as the inert substrate. The sample molecule was degassed under UHV, and the films are prepared on a clean substrate kept at 295K under the deposition rate of ~0.6nm/min. The experimental geometry is shown in Fig. 1 (b). The dependences of ARUPS on photoelectron emission angle (θ) were analyzed using multiple-scattering theory combined with molecular orbital (MST/MO) calculation [2]. We have calculated the θ pattern from a free molecule itself.

Results and Discussion

Figure 1 (c) shows the UPS of picene thick film (ca.10nm) on HOPG at photon energy ($h\nu$) of 28eV and $\theta=30^\circ$. We found six peaks A-F at the valence top region and they are represented well by the calculation for a free molecule, indicating the intermolecular interaction is very small in this film. These bands are all assigned to π MOs from the θ dependence (Fig. 2 (a)). The ionization energy of picene film is found to be 6.1eV.

The θ dependence of peak A (HOMO) in polar plot is shown in Fig.2 (b). Intensities of each peak are analyzed for the deconvoluted spectra where the contribution of HOPG substrate was subtracted because the thin film takes to form an island structure. The θ dependences of other peaks B-F are similar to that of HOMO, though they are categorized into two groups in the detailed pattern (not shown).

For the HOMO, the observed intensity gives the maximum at around 40° . The calculated intensities are evaluated for the molecular tilt angles β , which is inclined angle from the long-molecular axis, and γ , which is angle from the short axis (see the Fig. 1 (b)).

Azimuthal angle is integrated due to the polycrystalline sample. Among them, the $\gamma=\pm 5^\circ$ configuration gives the best agreement with the observed θ pattern. We found that most molecules are nearly flat to the substrates in the thin film phase.

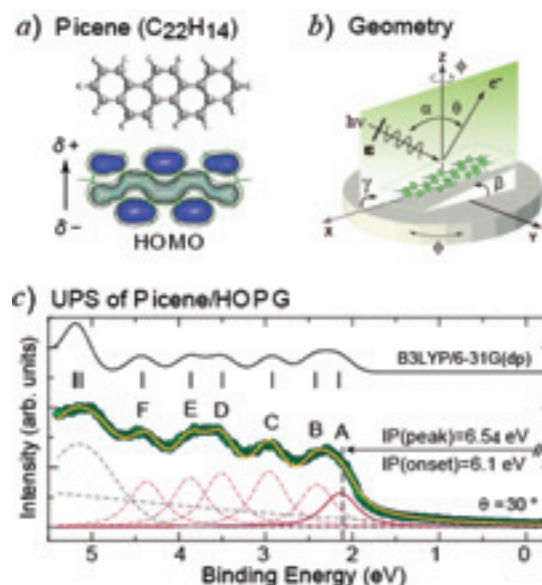


Fig. 1. a) Chemical structure and HOMO pattern of picene. b) Computation and experimental geometry for the MST/MO method. c) UPS of picene (10nm) film. The spectrum is convoluted with Voigt function. The calculated density-of-state and energy position of the molecular levels are also shown.

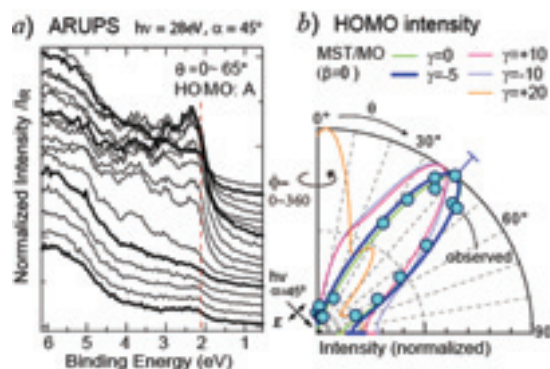


Fig. 2. a) θ dependence of ARUPS of picene film on HOPG. b) Observed and calculated θ patterns of the HOMO (peak A). The MST/MO results of the dependence on the molecular inclination angle of γ are shown for $\beta=0^\circ$.

[1] R. Mitsuhashi *et al*, Nature **464** (2010) 76.

[2] S. Nagamatsu *et al*, e-J. Surf. Sci. Nano, **3** (2005) 461.

Effects of Local Electrostatic Potential of Polar Molecule on Electronic Structure: ClGa-Phthalocyanine

H. Machida¹, S. Hosoumi¹, R. Tateishi¹, T. Nishi^{1,2}, S. Nagamatsu², T. Hosokai³, N. Ueno¹ and S. Kera^{1,2}

¹ Graduate School of Advanced Integration Science, Chiba University, Chiba 263-8522, Japan

² Institute for Molecular Science, Okazaki 444-8585, Japan

³ Institut für Angewandte Physik, Universität Tübingen, Germany

We investigated the electronic structure of chlorogallium phthalocyanine (ClGaPc) films on graphite. The electronic structure is significantly different between monolayer (ML) and bilayer (BL) at the HOMO band region especially. The effect of the local electrostatic potential of molecular permanent dipole on the interface electronic structure is an important subject to clarify the mechanism of the energy-level alignment. Angle-resolved ultraviolet photoelectron spectroscopy (ARUPS) measurements using synchrotron light source were conducted on ClGaPc/graphite system to reveal the effects of local and nonlocal electric field on the energy levels as well as the work function of the molecular film.

Experimental

The purified molecules were evaporated onto the graphite (HOPG) substrate kept at 295 K. The monolayer thickness was confirmed by the work function of the annealed monolayer film. The photoemission angle (θ) dependence was measured for HOMO band and Ga 3d band regions.

Results and Discussion

Figure 1 (a) shows the HeI UPS for the ML and BL of ClGaPc on HOPG at the HOMO band region. The spectra were fitted using Voigt function in accordance with hole-vibration(phonon) interaction [1]. For the ML film, the sharp asymmetric band A is assigned to the HOMO state with vibronic coupling. Unknown features at both sides of main band A are found (labeled as *). For the BL film, where the molecules are facing each other to compensate the permanent dipole, the HOMO is observed as two prominent bands (A' and B) with energy separation of 0.23eV. Band A' is related to photoemission from the underlying 1st layer, in which molecules are lying flat with Cl-atom protruding to vacuum side. Band B might be related to the 2nd layer, where molecules are oriented reversely as confirmed by the work function change and metastable atom electron spectroscopy [2]. Furthermore, θ dependences of band A and bands A' and B are shown in Figs. 1 (b) and (c), respectively. The observed intensities give the maximum at around 55° for every band as seen in other Pcs, indicating the same distribution of π MO as the origin of UPS bands.

To reveal the contribution of final-state screening of photohole on the UPS, which depends on the distance between the hole position and the image plane, we measured the Ga 3d state at $h\nu=80\text{eV}$ (Fig. 2 (a)). The Ga 3d-band shape is nearly the same

between ML and BL. θ dependences of Ga 3d peak for ML and BL show also no significant difference (Fig. 2 (b)), indicating the energy shift by the image potential is not the origin of the HOMO split.

The HOMO is delocalized over the Pc macrocycle, hence its orbital population may be affected by the electric field underneath. The results indicate that it is necessary to consider both the impacts of potential gradient by the local molecular dipole and the spontaneous polarization effect for a well-ordered staggered bilayer system.

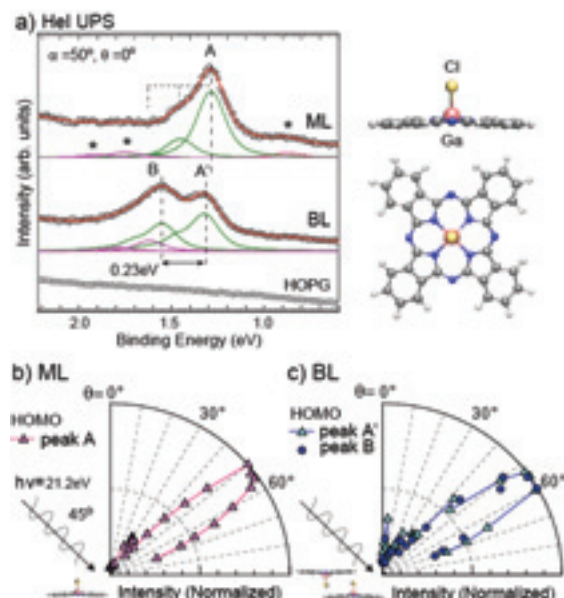


Fig. 1. (a) High-resolution UPS (HeI) of ClGaPc ML and BL on HOPG. (b) θ pattern of the HOMO for the ML and (c) for the BL.

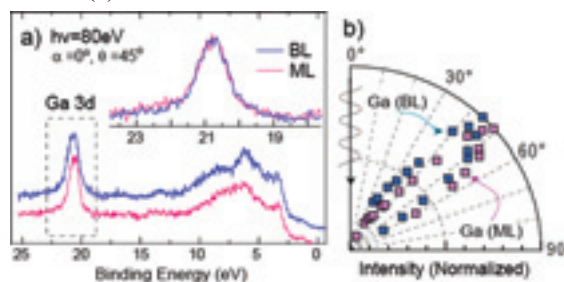


Fig. 2. (a) ARUPS at $h\nu=80\text{eV}$. Inset shows Ga band region. (b) θ pattern of the Ga3d for ML and BL.

[1] S. Kera *et al*, Prog. Surf. Sci. **84** (2009) 135.

[2] S. Kera *et al*, Surf. Sci. **566-568** (2004) 571.

Molecular Orientation at Organic-Organic Heterojunction Interfaces by ARUPS

K. K.Okudaira, K. Ito, N. Ueno

Association of Graduate Schools of Science and Technology, Chiba University, Inage-ku, Chiba 263-8522, Japan

Introduction

Organic field-effect transistors (OFETs) are of current interest due to their unique characteristics compared with those of conventional inorganic semiconductors. Because of the large size, anisotropy, and relatively weak van der Waals interaction of organic molecules, their growth is far more complex than that of inorganic materials. Studies on organic-inorganic heterojunction have revealed that the equilibrium structure is dependent on a delicate balance of various noncovalent weak interactions. Comparatively, the scenario of the rarely studied organic-organic interface (OOI) is much less understood. The investigation of structure of OOI may give information on the mechanism of the film growth at the OOI.

In this report we observed angle-resolved ultraviolet photoelectron spectroscopy (ARUPS) of pentacene (Pn) on organic thin film such as copper phthalocyanine (CuPc) and pentacene on HOPG to clarify the molecular orientation of OOI.

Experimental

ARUPS measurements were performed at the beam line BL8B2 of the UVSOR storage ring at the Institute for Molecular Science. The take-off angle (θ) dependencies of photoelectron spectra were measured at incident angle of photon (α) = 45° with the photon energy ($h\nu$) of 40 eV. CuPc thin film (1.6 nm) was first deposited on HOPG. An additional organic layer of pentacene was subsequently evaporated to a final thickness of 4.0 nm (Pn(4.0nm)/CuPc(1.6nm)/HOPG).

Results and Discussion

Figures 1 (a) and (b) show the take-off angle (θ) dependencies of ARUPS spectra of Pn(2.0nm)/HOPG and Pn(4.0nm)/CuPc(1.6nm)/HOPG, respectively. The peak located at binding energy of about 1 eV corresponds to the localized π state (HOMO). In Fig.2 the θ dependences of Pn(2.0nm)/HOPG have a sharp maxima at $\theta = 30^\circ$. These θ dependences are similar to those of CuPc on HOPG.[1] From these comparisons, it is found that Pn molecules lie flat on HOPG substrate. On the other hand, the θ dependences of Pn(4.0nm)/CuPc(1.6nm)/HOPG show broad distribution and have a maximum at $\theta = 60^\circ$, which is higher than that of Pn(2.0nm)/HOPG. We determined the orientation of pendant groups of polystyrene by the analysis of θ dependences of

ARUPS spectra.[2] These results indicate that Pn molecules on CuPc thin film show a tilt orientation. To determine the molecular orientation quantitatively, it needs to compare the observed θ dependencies with the calculated ones.

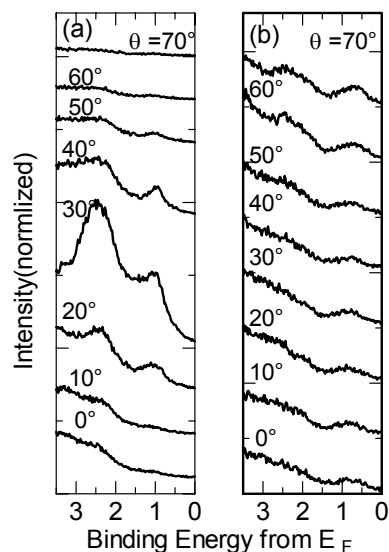


Fig.1. Take-off angle (θ) dependence of ARUPS of Pn(2.0nm)/HOPG (a), Pn(4.0nm)/CuPc(1.6nm)/HOPG (b), respectively.

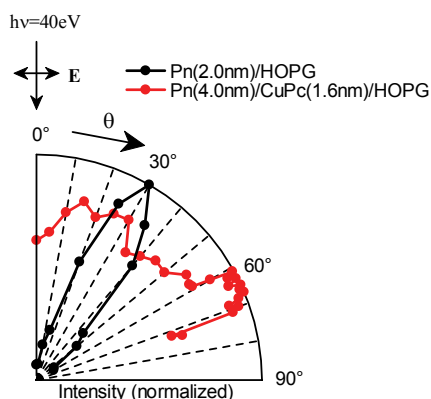


Fig.2. Take-off angle (θ) dependences of photoelectron intensities of HOMO peak for Pn(2.0nm)/HOPG (●) and Pn(4.0nm)/CuPc(1.6nm)/HOPG (●).

[1] K. K. Okudaira *et al.*, J. Appl. Phys **85** (1999) 6453.

[2] N. Ueno *et al.* Jpn. J. Appl. Phys. **37** (1998) 4979.

Effect of Insertion of a Thin Li-Phthalocyanine Layer at Indium Tin Oxide/Zn-Phthalocyanine Interface on Energy Level Alignment

S. Tanaka, T. Hanada and I. Hiromitsu

Department of Material Science, Interdisciplinary Faculty of Science and Engineering,
Shimane University, Matsue 690-8504, Japan

Introduction

The properties of metal-electrode/organic semiconductor interfaces affect the functionality and performance of organic semiconductor devices. An insertion of a thin layer in the metal-electrode/organic interfaces is a well known technique to improve the performance of organic semiconductor devices. [1] As an example of an interesting insertion effect on device performance, we recently observed that the power conversion efficiency of a Zn-phthalocyanine (ZnPc) /C₆₀ heterojunction organic photovoltaic (OPV) cell is improved with the insertion of a Li-phthalocyanine (LiPc) film to the indium tin oxide (ITO)/ ZnPc interface. The molecular structure of LiPc is shown in Fig. 1. It is known that the electronic structure of the ITO/organic interface is intimately related to the charge transfer properties of the ITO/organic layer. [2] Hence, in this study, we investigate the electronic structures of ITO/ZnPc and ITO/LiPc/ZnPc interfaces using photoelectron spectroscopy.

Experiment

The photoelectron measurements were carried out with photon energy of 40 eV. The incidence angle of light and the observed angle of the photoelectron were 45° and normal emission, respectively. The commercial ITO (supplied by Geomatec) substrate was cleaned with ultrasonication in organic solvents. LiPc was synthesized by electrochemical oxidation of dilithium phthalocyanine (Li₂Pc) following the synthesis procedure described in literature. [3] ZnPc was purchased from Kanto chem. co. LiPc and ZnPc were purified by vacuum sublimation. LiPc and ZnPc were deposited step by step at room temperature.

Results and Discussion

Figure 2 shows photoelectron spectra of LiPc and ZnPc incrementally deposited on the ITO substrate. The abscissa is the kinetic energy of the photoelectron. The Fermi level position of the ITO substrate was observed at 35.9 eV. The solid bars indicate the peak position of the highest occupied molecular orbital (HOMO) of LiPc and ZnPc at each sample thickness. The HOMO peak of LiPc was observed at 34.5 eV in 0.5 nm LiPc thickness. The HOMO peak of LiPc was settled at 34.7 eV with increasing the thickness of LiPc. The HOMO peak of ZnPc on the LiPc layer showed a 0.3 eV shift towards lower kinetic energy, indicating band bending in ZnPc due to the formation of an hole accumulation layer. The hole accumulation layer was not observed in the

thickness dependence of photoelectron spectrum of ZnPc at the ITO/ZnPc interface (not shown). In the OPV cell, ZnPc works as the path of the hole transport from the exciton dissociation interface. The present results indicate that the improvement of the power conversion efficiency is related to the band bending in the ZnPc layer caused by the insertion of the LiPc layer.

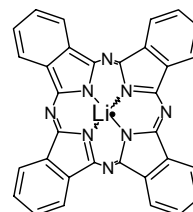


Fig. 1. Molecular structure of LiPc.

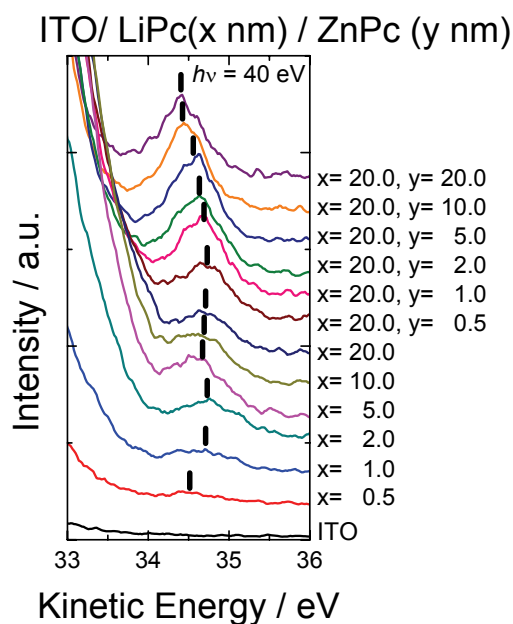


Fig. 2. Photoelectron spectra of LiPc and ZnPc incrementally deposited on the ITO substrate. The LiPc thickness and ZnPc thickness are indicated by the x and y in the right column, respectively.

[1] S. Tanaka *et al.*, *Thin Solid Films* **516** (2008) 1006.

[2] N. R. Armstrong *et al.*, *Thin Solid Films* **445** (2003) 342.

[3] P. Turek *et al.*, *Chem. Phys. Lett.* **134** (1987) 471.

Interface Electronic Structure of Co-Phthalocyanine/Cu(111)

R. Tateishi¹, S. Hosoumi¹, H. Machida¹, T. Nishi^{1,2}, S. Nagamatsu², N. Ueno¹ and S. Kera^{1,2}
¹Graduate School of Advanced Integration Science, Chiba University, Chiba 263-8522, Japan
²Institute for Molecular Science, Okazaki 444-8585, Japan

The interface electronic structure formed at an organic/electrode interface is of fundamental importance to understand mechanisms of charge injection and transfer phenomena in organic thin film devices, since they usually appear in the band gap region of the organic material. In general, however, it is very difficult to understand the mechanism of interface-states formation due to complicated and non-well-defined interface structure both in energetically and structurally. We studied on the valence electronic structure of cobalt-phthalocyanine (CoPc) thin films prepared on Cu(111) by using angle-resolved ultraviolet photoelectron spectroscopy (ARUPS).

Experimental

ARUPS spectra were measured at photon incidence angle $\alpha=45^\circ$, $h\nu=18$ and 40eV and $T=295\text{ K}$. The purified molecules were evaporated onto the Cu(111) substrate at 295 K . The coverage/thickness of the monolayer was confirmed by the work function of the densely-packed monolayer film. The high-resolution spectra were recorded by using HeI light source.

Results and Discussion

Figure 1 (a) shows the thickness-dependent ARUPS of CoPc (0.2nm; sub-monolayer(0.88ML) and 4.5nm) on Cu(111) obtained at $h\nu=40\text{eV}$. For the thicker film, the band A is ascribed to $2p$ (π) MO and B is from $3d$ - π hybridized MO of CoPc, respectively. For the thinner film, we found three interface states I1-I3. The energies of bands I2 and I3 are slightly higher ($\delta\sim 0.05\text{eV}$ and 0.18eV) than that for the CoPc/Ag(111), respectively. A modified Shockley-surface state (SS) is also observed at around $\theta=0^\circ$.

The intensity map for the ARUPS along the ΓM direction of CoPc(0.2nm)/Cu(111) is shown in Fig. 1 (b). No clear energy-band dispersion is found for valence states of CoPc film. The photoelectron angular distribution (PAD) of bands I2 and I3 are accidentally similar each other at $h\nu=40\text{eV}$, where each curve has a maximum at $\sim 34^\circ$. On the other hand, we found similarities of the PADs between CoPc/Cu(111) and CoPc/Ag(111). By considering the systematic changes in the electronic structure for various transition-metal Pcs, band I2 is ascribed to the $3d$ -related MO and I3 is from the $2p$ -related MO. Band I1 might be described to an adsorption-induced gap state. The re-ordering and modification of MOs is keys to understand the formation mechanism of the interface states.

Figure 2 shows the evolution of SS of Cu(111) with increasing the coverage of CoPc. The peak energy at Γ point shifts to lower energy side with increasing the coverage (see a guided curve). The characteristics of

the modified SS are that (i) the SS at uncovered region disappears for subML films and (ii) the electron mass (m^*) tends to be heavier with increasing the coverage. This tendency clearly differs from the case of rare gases adsorption. The SS at the bare surface region survives and m^* of the modified SS does not changed so much for Xe/Cu(111) [1].

A peculiar interaction between organic molecule and metal as well as a film growth process should take part in. The study to obtain the detailed structural information on lattice constant by LEED as well as adsorption distance by XSW that depends on the coverage is in progress.

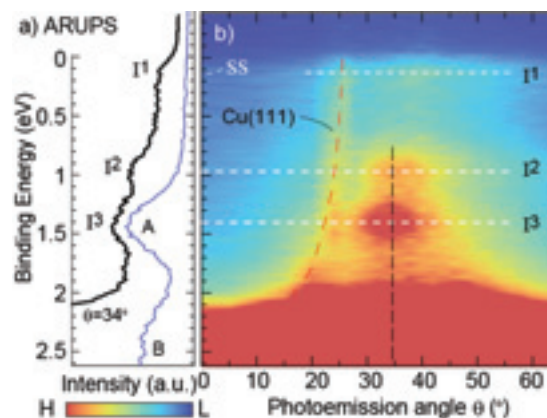


Fig. 1. a) Thickness-dependent ARUPS of CoPc/Cu(111), subML(black) and thick film(blue). b) Intensity map for the θ dependence of ARUPS at the subML. The band dispersion of the Cu(111) is overlapping (see a dashed curve).

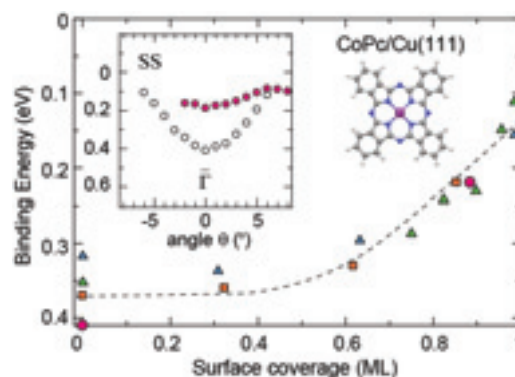


Fig. 2. Thickness dependence of the SS peak position (Γ point). Results of three different experiments by HeI UPS are compared. Inset shows ARUPS of clean Cu(111) (open circles) and CoPc(0.88ML)/Cu(111) (filled circles) taken at $h\nu=18\text{eV}$.

[1] F. Forster *et al.*, J. Phys. Chem. B **108** (2004) 14692.